

IQGAP1 mediates podocyte injury in diabetic kidney disease by regulating nephrin endocytosis

Yipeng Liu^a, Hong Su^{a,b}, Chaoqun Ma^c, Dong Ji^d, Xiaoli Zheng^c, Ping Wang^a, Shixiang Zheng^e, Li Wang^a, Zunsong Wang^a, Dongmei Xu^{a,*}

^a Department of Nephrology, Shandong Provincial Qianfoshan Hospital, Shandong University, Jinan 250014, China

^b Department of Nephrology, Shandong Provincial Hospital Affiliated to Shandong University, Jinan 250021, China

^c Department of Emergency, Shandong Provincial Hospital Affiliated to Shandong University, Jinan 250021, China

^d Department of Dialysis, Huimin County People's Hospital, Binzhou 251700, China

^e Division of Critical Care Medicine, Union Hospital of Fujian Medical University, Fuzhou 350001, China

ARTICLE INFO

Keywords:

IQ domain GTPase-activating protein 1
Nephrin
Endocytosis
Podocyte injury
Diabetic kidney disease

ABSTRACT

Diabetic kidney disease (DKD) is a complication associated with diabetes and is a major public health problem in modern society. Podocyte injury is the central target of the development of DKD, and the loss or dysregulation of nephrin, a key structural and signalling molecule located in the podocyte slit diaphragm (SD), initiates potentially catastrophic downstream events within podocytes. IQGAP1, a scaffold protein containing multiple protein-binding domains that regulates endocytosis, can interact with nephrin in podocytes. It is hypothesized that IQGAP1 contributes to nephrin endocytosis and may participate in the pathogenesis of DKD. The dramatically increased histo-nephrin granularity score in DKD glomeruli showed a significant positive correlation with increased IQGAP1-nephrin interaction without changes in the total protein content of nephrin and IQGAP1. In cultured human podocytes, hyperglycaemia induced the intracellular translocation of IQGAP1 from the cytosol to the vicinity of the cytomembrane, reinforced the IQGAP1-nephrin interaction, and augmented nephrin endocytosis. Moreover, impaired podocyte function, such as migration, extensibility and permeability, were further aggravated by wild-type IQGAP1 plasmid transfection, and these effects were partially restored by siRNA-mediated IQGAP1 downregulation. Collectively, these findings show that IQGAP1, an intracellular partner of nephrin, is involved in nephrin endocytosis and the functional regulation of podocytes in DKD.

1. Introduction

The number of patients with diabetes has increased, and the estimated prevalence of diabetes is 12% to 14% among adults in the U.S [1]. Notably, patients with diabetes are at a particularly high risk for chronic kidney disease (CKD) and its sequelae; the prevalence of CKD among individuals with diabetes is > 40% compared with ~10% in the general U.S. adult population [2], and the presence of CKD is an important contributor to the increased mortality associated with diabetes, which has a 10-year cumulative all-cause mortality of 31.1% [3]. The appearance of progressively increasing albuminuria is the hallmark of diabetic kidney injury, resulting from glomerular filtration barrier damage. Podocytes are terminally differentiated cells that form the slit diaphragm (SD), which is an essential component of the glomerular filtration barrier. SD molecules, adapter proteins and cytoskeleton

elements form a tight network to stabilize filtration barrier function, and defects in these components permit proteinuria [4,5].

Nephrin, as the first described transmembrane protein located in the SD, is involved in many signalling transduction processes and has an important biological function in podocytes [6]. Many studies have confirmed that changes in the expression or distribution of nephrin could lead to the loss of the structure and function of the SD and result in massive proteinuria and renal failure [7]. Furthermore, the transposition of nephrin from the cytomembrane to cytosol has been detected in diabetic kidney disease (DKD) [8]. In addition, recent evidence has suggested that endocytosis may play a vital role in the rapid downregulation of cell surface nephrin expression and the destruction of SD integrity [9]. However, the potential mechanism of nephrin endocytosis in podocytes is not well understood.

IQ domain GTPase-activating protein 1 (IQGAP1) is a scaffold

* Corresponding author at: Department of Nephrology, Shandong Provincial Qianfoshan Hospital, Shandong University, No.16766, Jingshi Road, Jinan 250014, China.

E-mail address: xudongmei@sdhospital.com.cn (D. Xu).

<https://doi.org/10.1016/j.cellsig.2019.03.009>

Received 2 October 2018; Received in revised form 7 March 2019; Accepted 8 March 2019

Available online 09 March 2019

0898-6568/© 2019 Elsevier Inc. All rights reserved.

protein containing multiple protein-binding domains that acts as a polymerization platform for a variety of protein molecules and signalling kinases. Previous studies have shown that IQGAP1 plays a core role in regulating the internalization of multiple membrane proteins [10,11]. The interaction between IQGAP1 and nephrin has been discovered in 2005 by Farquhar and Tryggvason research groups [12,13]. And our previous study published in 2014 demonstrated that IQGAP1 co-locates with nephrin in podocytes and acts as an intracellular partner of nephrin in puromycin aminonucleoside nephrosis [14]. However, the role of IQGAP1 in DKD has not been reported. Thus, in the present study, we evaluated the role of IQGAP1 in mediating the mislocalization of nephrin in DKD.

2. Materials and methods

2.1. Human renal biopsy samples

Renal biopsy had been performed as a routine clinical operation. Renal tissues with pathological diagnosis of DKD were used as experimental samples, and control samples were obtained from the healthy kidney poles of patients who underwent nephrectomy for solitary renal carcinoma without other renal diseases. These investigations were approved by the Ethics Review Committee of Shandong Provincial Qianfoshan Hospital, Shandong University and were implemented according to the Declaration of Helsinki. All participants provided written informed consent.

2.2. Animals

All experimental procedures were approved by the Ethics Committee for Animal Experiments of Shandong Provincial Qianfoshan Hospital, Shandong University. Seventeen male SPF C57BL/6 mice were supplied by the Experimental Animal Center of Shandong University and raised in a temperature- and humidity-controlled laminar flow room under a 12 h light/12 h dark cycle with free access to water and food. After 3 days of adaptive feeding, the DKD model was established by unilateral nephrectomy and then intraperitoneal injection of streptozotocin (80 mg/kg/d, Sigma-Aldrich, USA) for 3 days. All mice were maintained on a high-fat diet for 12 weeks, in accordance with the study by Liu et al [15]. The mice were weighed weekly, and serum glucose was measured weekly with a Glucometer Elite (Bayer, Germany). At the end of the study, body weight, blood pressure (determined by tail-cuff plethysmography, Harvard Apparatus, USA), serum creatinine (determined by a Cobus 8000 Analyser, Roche Diagnostics GmbH, Switzerland), and serum glucose were measured. Urine was collected for 24 h in a metabolic cage, and the urinary protein-to-creatinine ratio was measured by a Cobus 8000 Analyser (Roche Diagnostics GmbH, Switzerland). The mice were sacrificed with 10% chloral hydrate. Part of the kidney was applied for the isolation of glomeruli [14] and then used for co-immunoprecipitation and Western blotting analyses. The cortex of the rest of the kidney was separated and fixed in 4% phosphate-buffered paraformaldehyde, glutaraldehyde, or tissue-freezing medium for renal pathological and immunofluorescence analysis.

Transmission electron microscopy (Hitachi H-600, Japan) was used to evaluate the ultrastructural changes in podocytes, and the mean foot process (FP) width was defined as the total length of the glomerular basement membrane (GBM) divided by the total number of FPs. The FP fusion rate was presented as the length of FP fusion divided by the total length of the GBM.

2.3. Cell culture

Conditionally immortalized human podocytes were originally provided by Dr. Moin A. Saleem (Academic Renal Unit, Southmead Hospital, Bristol, UK) and cultured in RPMI 1640 medium (HyClone,

USA) containing 10% foetal bovine serum (Gibco, USA) and $1 \times$ penicillin-streptomycin in a 5% CO₂ incubator. The cells were subcultured at 33 °C during the proliferation phase and then cultured in a 37 °C incubator for 7 days to induce differentiation. The differentiated cells were incubated with normal glucose (Control, 5.5 mM) or high glucose (HG). The cells in the HG condition were stimulated with variable concentrations of glucose (10–40 mM) for different times (0–24 h). Additionally, 40 mM mannitol was used as an osmotic pressure control.

Human glomerular endothelial cells (HRGECs), human glomerular mesangial cells (HRMCs) and a proximal tubular epithelial cell line (HK-2) were provided by Dr. Yi Fan (Department of Pharmacology, Shandong University School of Medicine, Jinan, China) and cultured as described [16].

2.4. Regulation of gene expression

The expression plasmid of full-length IQGAP1 (pCAN-myc-IQGAP1) was originally provided by Dr. Jon Erickson (Cornell University, NY, USA). For plasmid transfection, differentiated podocytes were incubated with transfection complexes containing 2.5 µg of plasmid and 7.5 µL of Lipofectamine 3000 Transfection Reagent (Invitrogen, USA) under growth conditions for 72 h.

IQGAP1 siRNA (target sequence: GCAGGTGGATTACTATAAA) was synthesized by RIBOBIO Biotechnology Co., Ltd. (China) and transfected according to the manufacturer's instructions. In short, the differentiated podocytes were incubated with transfection complexes containing 5 µL of siRNA and 12 µL of riboFECT™ CP transfection reagent under growth conditions for 48 h.

2.5. Real-time PCR

Total RNA was extracted using TRIzol reagent (Invitrogen, USA), and the concentration was measured by spectrophotometry. After cDNA was synthesized, real-time fluorescent quantitative PCR was performed (ABI VIIA7, USA). Specificity was determined by melting-curve analysis, and β-actin was used as an internal reference. The primers used in our study were as follows: IQGAP1 sense, 5'-GGGGAAACGTACCAGAG TGA-3' and anti-sense, 5'-TCTCGAGAAAGCTGCACAGA-3'; β-actin sense, 5'-CACGATGGAGGGCCGACTCATC-3' and anti-sense, 5'-TAA AGACCTCTATGCCAACACAGT-3'.

2.6. Immunofluorescence staining

For histoimmunofluorescence analysis, frozen kidney sections (5 µm thick) were blocked with 5% BSA for 30 min at 37 °C, incubated with nephrin guinea pig primary polyclonal antibody (pAb, 1:50; PROGEN Biotechnik, Germany) overnight at 4 °C, and then incubated with a FITC-conjugated goat anti-guinea pig IgG secondary antibody (1:100, Santa Cruz, USA) at 37 °C for 90 min in the dark.

For immunocytofluorescence analysis, cells grown on glass slides were fixed with 4% paraformaldehyde for 30 min at 4 °C and then co-incubated with nephrin guinea pig primary pAb (1:50; PROGEN Biotechnik, Germany) and IQGAP1 rabbit primary pAb (1:50; Santa Cruz, USA) overnight at 4 °C. FITC-conjugated goat anti-guinea pig IgG (1:100, Santa Cruz, USA) and TRITC-conjugated goat anti-rabbit IgG (1:100, Santa Cruz, USA) antibodies were subsequently used for multi-labelling immunodetection.

Finally, all the samples were examined using a confocal fluorescence microscope (LSM780, Carl Zeiss, Germany) and analysed using ZEN system 2012 (Carl Zeiss, Germany). For histo-nephrin granularity scoring, randomly selected glomeruli images of each mouse were scored from 0 (smooth) to 5 (granular) based on the overall granularity of the nephrin staining.

2.7. Cytomembrane protein extraction

The podocyte membrane proteins were extracted using a membrane protein extraction kit (Beyotime Biotechnology, China). Briefly, the fully homogenized cell debris was centrifuged at $700 \times g$ for 10 min at 4°C , and then, the supernatant was centrifuged at $14000 \times g$ for 30 min at 4°C to precipitate the cytomembrane debris. After discarding the supernatant, cytomembrane protein extraction reagent was added to the sediment to complete the extraction process.

2.8. Western blotting

The protein concentration was measured using an enhanced BCA protein assay kit (Beyotime Biotechnology, China). Equal quantities of denatured protein in loading buffer were separated using 10% SDS-PAGE and then electrophoretically transferred to polyvinylidene fluoride membranes (Millipore, USA). The membranes were incubated with primary antibodies (nephrin rabbit pAb, 1:200, Santa Cruz, USA; IQGAP1 rabbit pAb, 1:200, Santa Cruz, USA; β -actin mouse mAb, 1:1000, Santa Cruz, USA; plasma membrane loading control Na⁺/K⁺-ATPase rabbit mAb, 1:100000, Abcam, UK) overnight at 4°C followed by incubation with a horseradish peroxidase-conjugated anti-rabbit or anti-mouse IgG (1:10000, Cell Signalling Technology, USA), respectively. Bands were visualized by ECL reagent (Santa Cruz, USA), and the integrated optical density of each band was calculated using ImageJ.

2.9. Co-immunoprecipitation

Total protein from glomeruli and cultured podocytes was extracted using lysis buffer (1 mM PMSF, 5 mM EDTA, 1.0% Triton X-100, 150 mM NaCl, 20 mM Tris, pH 7.5) containing a protease inhibitor cocktail (P8340, Sigma-Aldrich, USA). The samples were centrifuged at $13,000 \times g$ for 5 min at 4°C , nephrin rabbit pAb ($2 \mu\text{g}/500 \mu\text{g}$ total protein; Santa Cruz, USA) was added to the supernatants, and the mixtures were rotated overnight at 4°C . Then, the mixtures were loaded with protein A + G agarose (Beyotime Biotechnology, China) and incubated for 3 h at 4°C . The centrifuged sediment was saved and mixed with $1 \times$ LDS sample buffer. After boiling at 95°C for 10 min, the samples were analysed by Western blotting.

2.10. Immunocytofluorescence-based internalization assay

The FM4-64 uptake experiment was carried out to study internalization. Briefly, podocytes plated on glass slides were serum starved for 1 h and then incubated with an endocytic marker, FM4-64 (PromoKine, Germany), at 4°C for 30 min. After the induction of internalization at 37°C for 30 min, cells were fixed with 4% paraformaldehyde, permeabilized with 0.1% Triton, incubated with nephrin guinea pig primary pAb (1:50; PROGEN Biotechnik, Germany) overnight at 4°C , and then incubated with a FITC-conjugated goat anti-guinea pig IgG second antibody (1:100, Santa Cruz, USA) at 37°C for 90 min in the dark. The samples were examined using a confocal fluorescence microscope (LSM780, Carl Zeiss, Germany) and analysed using ZEN system 2012 (Carl Zeiss, Germany).

2.11. Podocyte functional assay

The migration and extensibility assays were performed as described previously [14]. Briefly, for the migration assay, pictures were taken with an inverted phase contrast microscope just before (0 h) and 24 h after scraping. To estimate cell migration, the number of cells crossing the $100 \mu\text{m}$ wound border was calculated.

For the extensibility assay, the morphology of podocytes was observed after 6 h under an inverted phase contrast microscope. Spread cells had extended processes, whereas unspread cells were round. The

percentage of spreading podocytes was defined as the number of spread cells divided by the total number of cells.

For the permeability assays, cells were inoculated into the upper chamber of a Transwell insert ($0.4 \mu\text{m}$, Corning, USA) and cultured until confluent. The chambers were washed with HEPES medium, and 1 mg of 70 kDa FITC-dextran (Invitrogen, USA) in 1 mL of PBS was added to the upper chamber. After 4 h, samples were collected from the bottom chamber and read in a fluorometer at an excitation wavelength of 485 nm and emission wavelength of 520 nm.

2.12. Statistical analysis

The values are presented as the mean \pm SD, and statistical analysis was performed using SPSS ver. 19.0. The statistical comparison between control and DKD mice was conducted using independent *t*-tests. Statistical comparisons among multiple groups were conducted using one-way ANOVA, and the LSD test was used for multiple comparisons. $P < 0.05$ indicated statistical significance.

3. Results

3.1. Mislocalization of nephrin in the glomeruli of patients and mice with DKD

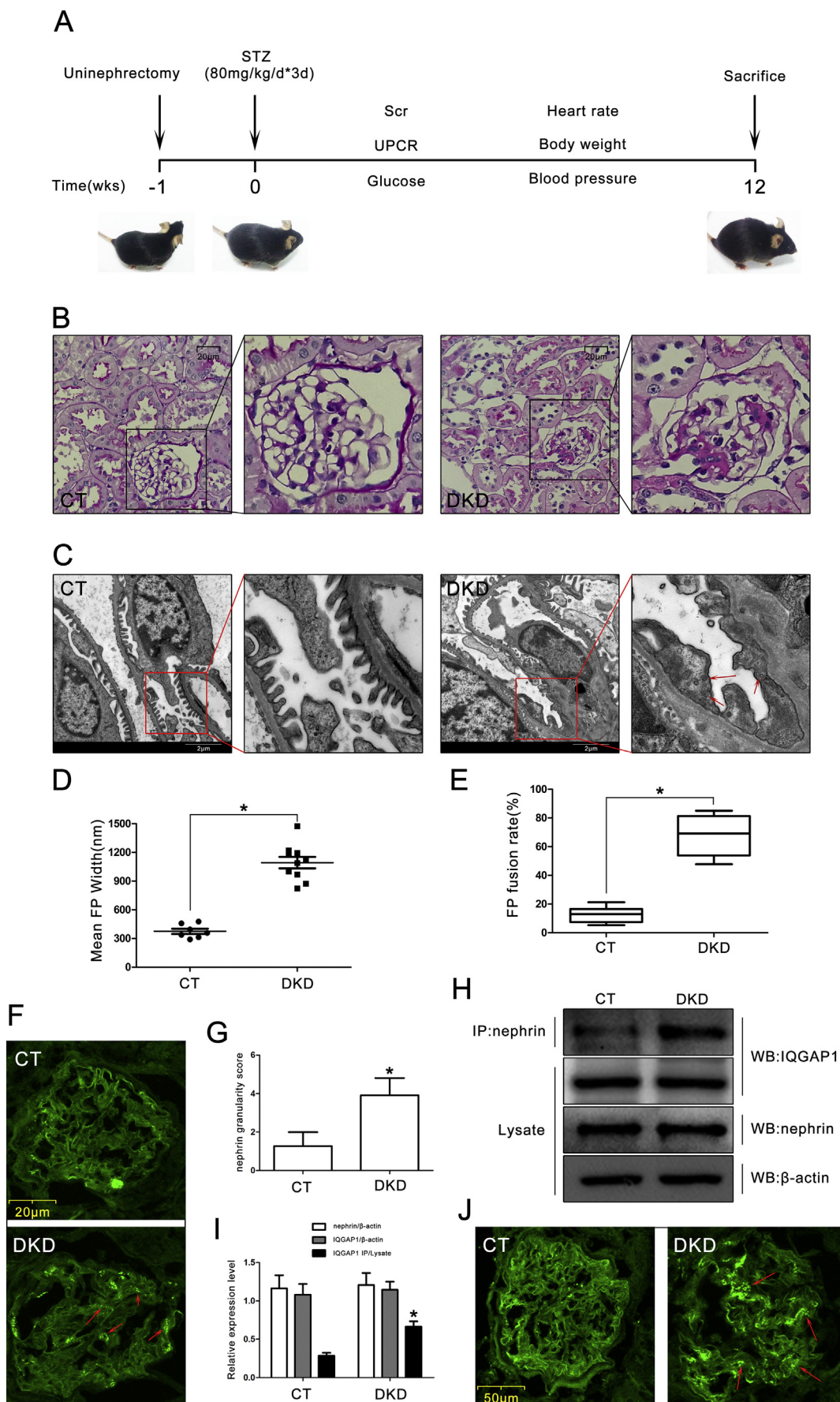
We established a mouse model of DKD (Fig. 1A) to investigate the pathogenesis of FP fusion and proteinuria. Biochemical indicators and Periodic acid–Schiff (PAS) staining (Table S1 and Fig. 1B) showed that the DKD model was successfully established. Ultrastructural analysis of podocytes (Fig. 1C, D, E) indicated that the mean FP width and FP fusion rate were increased in the DKD group compared with the control group, and interestingly, we also detected many endocytic vesicles in the SD region of podocyte FPs in DKD mouse glomeruli. Next, we performed immunofluorescence and Western blotting to detect the localization and expression of nephrin in glomeruli. As shown in Fig. 1F, the smooth linear distribution of nephrin along the capillary loops that was observed in controls was altered to a diffuse granular appearance under diabetic conditions, without a change in total protein content (Fig. 1H, I); this phenomenon was also observed in human kidney tissue (Fig. 1J). In addition, the IQGAP1–nephrin interaction in glomeruli was clearly increased in DKD mice compared with control mice (Fig. 1H, I), and interestingly, the IQGAP1–nephrin interaction showed a significant positive correlation with the granularity score of nephrin staining (Spearman $r = 0.872$, $P < 0.01$) (Fig. 1G).

3.2. The expression level of IQGAP1 in podocytes is not altered under hyperglycaemic conditions

We first detected the expression of IQGAP1 in different renal cells, such as podocytes, HK-2 cells, HRMCs and HRGECs. The results indicated that the HRGECs and podocytes had a significantly higher expression level of IQGAP1 relative to HRMCs, as shown in Fig. 2A and B. Moreover, by means of immunohistochemical detection (Fig. 2C), we found that IQGAP1 was widely expressed in the glomeruli and that the pathological state of DKD did not affect IQGAP1 expression intensity in podocytes. Next, we detected IQGAP1 expression in podocytes under hyperglycaemic conditions and found that the expression level of IQGAP1 was comparable at different stimulus concentrations and times (Fig. 2D, E, F, G, H, I).

3.3. The interaction between IQGAP1 and nephrin in podocytes is enhanced under hyperglycaemic conditions

The significant positive correlation between the nephrin granularity score and the IQGAP1–nephrin interaction in glomeruli impelled us to further explore the potential role of the IQGAP1–nephrin interaction in hyperglycaemia. The results indicated that hyperglycaemic conditions



(caption on next page)

Fig. 1. Expression and localization of nephrin in the glomeruli of patients and mice with DKD. (A) The process of DKD mouse model construction. (B) Representative microscopy images of renal pathological changes in two groups (PAS staining, original magnification, $\times 200$). Scale bar = 20 μm . (C) Representative transmission electron microscopy images of glomerular podocyte FPs (original magnification, $\times 10,000$), and quantitative analysis of the FP width (D) and FP fusion rate (E) (CT $n = 7$, DKD $n = 10$). The arrow indicates the endocytic vesicle in the SD region of podocyte FPs. Scale bar = 2 μm . (F) Representative immunofluorescence images of nephrin localization in DKD mouse glomeruli (original magnification, $\times 400$). The arrow indicates the granular distribution patterns of nephrin. Scale bar = 20 μm . (G) Scoring of the granularity of nephrin staining in DKD mouse glomeruli (CT $n = 7$, DKD $n = 10$). (H) (I) Western blotting analysis of glomerular nephrin and IQGAP1 expression and co-immunoprecipitation analysis of nephrin and IQGAP1 in two groups (CT $n = 7$, DKD $n = 10$). (J) Representative immunofluorescence images of nephrin localization in glomeruli of patients with DKD (original magnification, $\times 400$). The arrow indicates the granular distribution patterns of nephrin. Scale bar = 50 μm . * $P < 0.05$ relative to controls.

significantly increased the level of IQGAP1 and nephrin co-immunoprecipitation in a dose- (Fig. 3A, B) and time-dependent (Fig. 3C, D) manner, excluding the effect of osmotic pressure with mannitol. Next, we performed double immunolabelling to detect the distribution of nephrin and IQGAP1 in cultured podocytes under hyperglycaemic conditions. As shown in Fig. 3E, under normal conditions, nephrin mainly resided in the cytomembrane, and IQGAP1 was mainly distributed in the cytosol. After high-glucose (20 mM, 40 min) stimulation, IQGAP1 accumulated in the vicinity of the cytomembrane and colocalized with nephrin; moreover, most of the nephrin was transported from the cytomembrane to the cytosol.

3.4. The IQGAP1-nephrin interaction is influenced by the regulation of endogenous IQGAP1 in podocytes

We used an IQGAP1 plasmid and siRNA to regulate the endogenous expression of IQGAP1 in cultured podocytes, and then, the expression of IQGAP1 was examined by Western blotting analysis. As shown in the results, the IQGAP1 wild-type plasmid dramatically increased IQGAP1 expression (Fig. 4A, B) whereas the IQGAP1 siRNA significantly decreased IQGAP1 expression (Fig. 4C, D) compared to that in control podocytes ($P < 0.05$), which indicated successful interference with IQGAP1 expression. However, while the expression of nephrin was not affected in IQGAP1 plasmid- or siRNA-transfected cells, the interaction between IQGAP1 and nephrin was significantly influenced: the quantity of IQGAP1 co-immunoprecipitated with nephrin increased significantly with the upregulation of IQGAP1 expression and decreased remarkably with the downregulation of IQGAP1 expression compared with control levels (Fig. 4E, F).

3.5. IQGAP1 is involved in the functional regulation of podocytes

To further explore the role of IQGAP1 in podocytes, we designed and conducted a series of experiments to test parameters such as cell migration, extensibility and permeability. As shown in Fig. 5, podocyte migration and extensibility were inhibited, but permeability was provoked noticeably under hyperglycaemic conditions. Furthermore, the trends observed in migration, extensibility and permeability were partially recovered by transfection with IQGAP1 siRNA and progressively worsened by IQGAP1 overexpression.

3.6. IQGAP1 plays an important role in nephrin endocytosis

To assist in evaluating nephrin endocytosis, we labelled endocytic vesicles in live cells with FM4-64, and then, nephrin antibody was used for double fluorescent labelling. As shown in the results, compared with those in normal cells, the podocytes treated with 20 mM glucose for 40 min had more endocytic vesicles; moreover, the colocalization of nephrin with these granular vesicles was clearly increased, which indicated a significant increase in nephrin endocytosis. Additionally, IQGAP1 overexpression dramatically increased the colocalization of nephrin with FM4-64-labelled endocytic vesicles compared with that in high-glucose-stimulated cells, while the level of colocalization was partially recovered when IQGAP1 siRNA transfection was conducted (Fig. 6A). In addition, we extracted podocyte membrane proteins and examined the nephrin content by Western blotting to further detect the

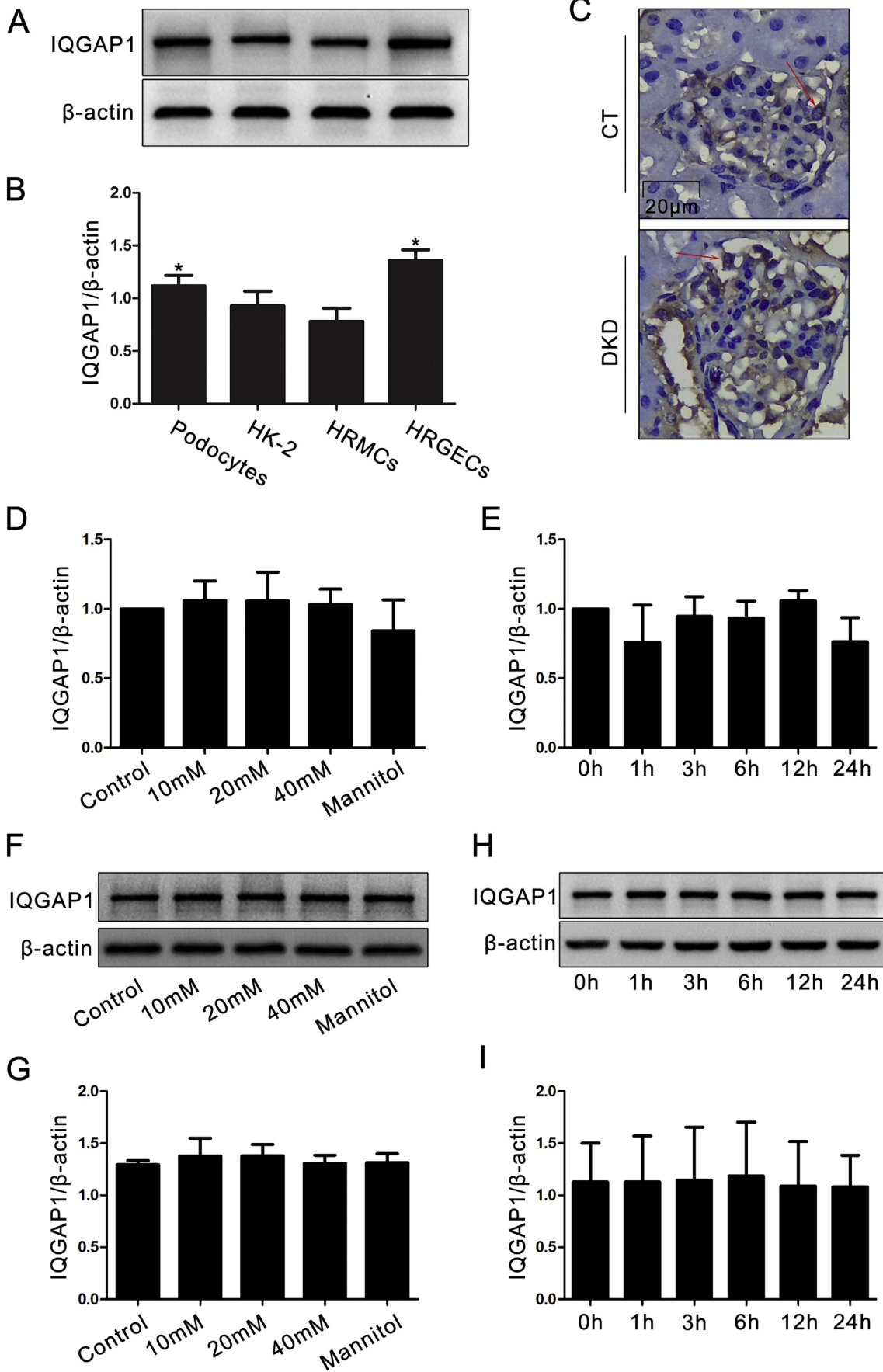
endocytosis of nephrin under different conditions. The results showed that the content of nephrin in the cytomembrane was significantly decreased in cells under hyperglycaemic conditions compared with those under normal conditions. Furthermore, overexpression of IQGAP1 caused a significant reduction in cytomembrane nephrin content compared with control treatment, while the content of cytomembrane nephrin was dramatically recovered to nearly normal levels when IQGAP1 siRNA transfection was conducted (Fig. 6B, C).

4. Discussion

DKD is one of the most important microvascular complications of diabetes and is characterized by proteinuria and progressive loss of kidney function. It is virtually the leading cause of end-stage renal disease in Western countries, and its incidence increases each year in China [17]. As DKD is a classic podocytopathy, the research on its pathogenesis has gradually focused on podocyte injury, which is characterized by FP fusion [18,19]. In our study, we established a DKD mouse model to explore the potential mechanism of podocyte injury under diabetic conditions. In addition to the characteristic features of proteinuria and FP effacement, a concomitant increase in endocytic vesicles in the SD region of podocyte FPs and alterations in the nephrin distribution pattern from a smooth linear distribution along the capillary loops in controls to a diffuse granular appearance in DKD were also observed, implying a contribution of endocytosis to the pathogenic changes in podocytes in DKD.

Endocytosis is an elementary process by which cells internalize membrane-bound components, such as transmembrane proteins, hormones, and growth factors, to special compartments in the cytosol to regulate relevant signalling pathways. Emerging studies have confirmed that endocytic trafficking allows rapid regulation of the signalling strength at the SD [20]. The first described SD molecule, nephrin, which is a transmembrane protein with a short intracellular domain, a single-span transmembrane region and a large extracellular domain with eight distal Ig-like motifs and a proximal fibronectin type III domain [21], is not only an essential structural component of the SD filtration network but also a signalling hub controlling podocyte adhesion, mobility and survival [22]. Currently, many studies have suggested that nephrin is mislocalized during podocyte injury [23–25], and although nephrin endocytosis appears to be a tightly regulated process, the overabundance of nephrin endocytosis may initiate potentially catastrophic downstream events within podocytes [26,27]. In the present study, hyperglycaemia in cultured podocytes induced the translocation of nephrin from its basal location on the surface of the cytomembrane to the cytosol, increased the colocalization of nephrin with FM4-64-labelled endocytic vesicles, and decreased the content of nephrin in the cytomembrane; furthermore, concomitant impairment of podocyte functions such as migration, extensibility and permeability were detected. All of the above results collectively verified that nephrin is over-endocytosed during the pathogenic changes that occur in podocytes in DKD. Although several proteins such as Notch [28], CIN85 [23], beta-arrestin [29], PACSIN2 [30] and ShcA [24], have been reported to be involved in nephrin endocytosis, the exact mechanisms about nephrin mislocalization in DKD still need in-depth study.

Scaffold proteins serve as a polymerization platform for many kinds of molecules and signal-related kinases and are responsible for targeted



(caption on next page)

Fig. 2. Expression of IQGAP1 in podocytes under hyperglycaemic conditions. (A) (B) Western blotting analysis of IQGAP1 expression in podocytes, HK-2, HRMCs and HRGECs ($n = 3$). $*P < 0.05$ relative to HRMCs. (C) Representative immunohistochemistry images of IQGAP1 expression in DKD mouse glomeruli (original magnification, $\times 400$). Scale bar = $20 \mu\text{m}$. The red arrows indicate IQGAP1 expression in podocytes. (D) (E) Real-time PCR analysis of IQGAP1 expression in cultured podocytes stimulated by various concentrations of glucose for 24 h or by 20 mM glucose for 0–24 h ($n = 3$). (F) (G) (H) (I) Western blotting analysis of IQGAP1 expression in cultured podocytes treated with high glucose ($n = 3$). 40 mM mannitol was used as an osmotic pressure control. (For interpretation of the references to colour in this figure legend, the reader is referred to the web version of this article.)

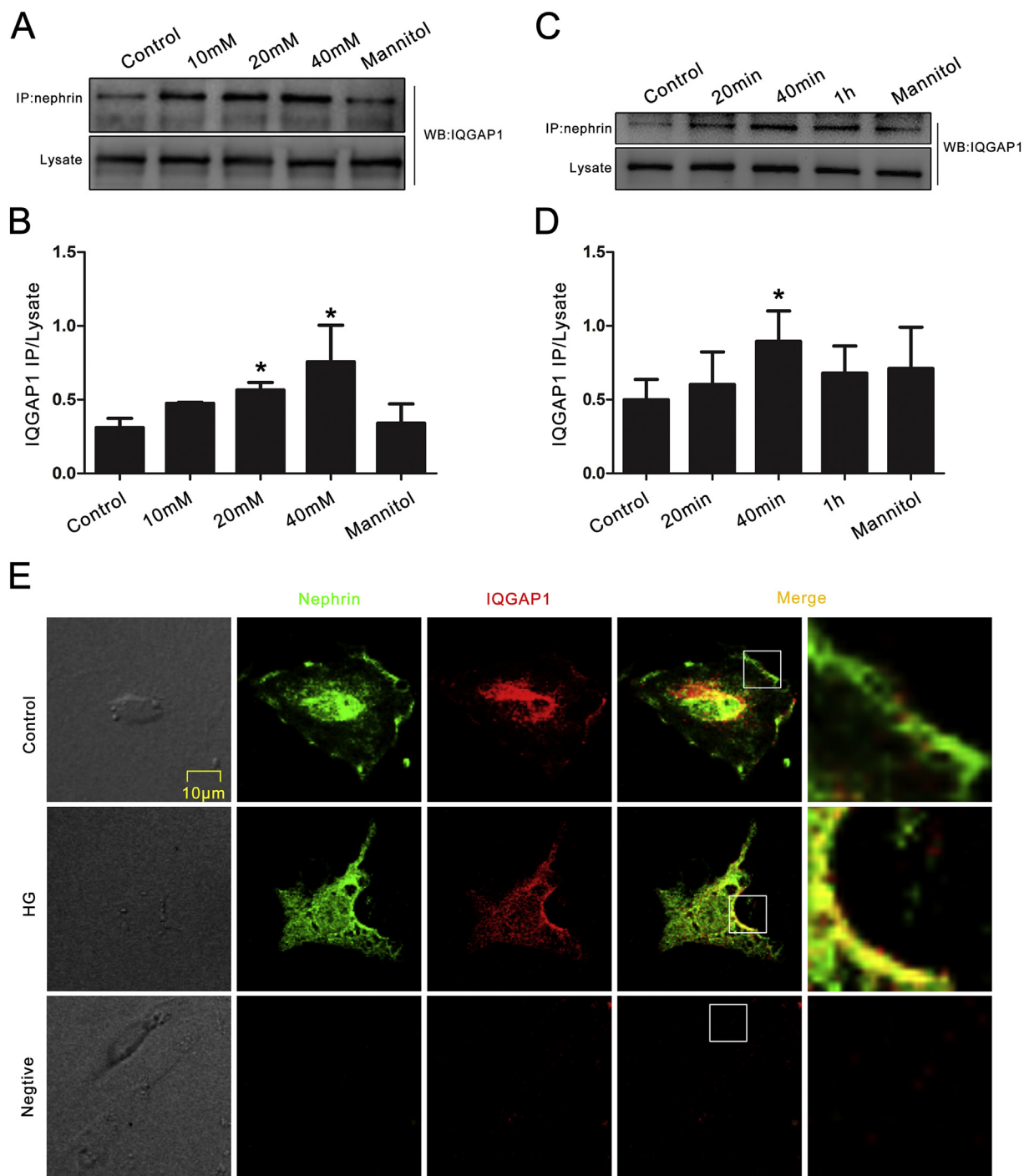


Fig. 3. Interaction between IQGAP1 and nephrin in high-glucose-stimulated podocytes. (A) (B) Co-immunoprecipitation analysis of IQGAP1 and nephrin in podocytes treated with various concentrations of glucose for 40 min. 40 mM mannitol was used as an osmotic pressure control ($n = 3$). (C) (D) Co-immunoprecipitation analysis between IQGAP1 and nephrin in podocytes treated with 20 mM glucose for 0–1 h. The same concentration of mannitol was used as an osmotic pressure control ($n = 3$). (E) Double immunolabelling of nephrin and IQGAP1 in cultured podocytes with high-glucose stimulation (original magnification, $\times 400$). Scale bar = $10 \mu\text{m}$. $*P < 0.05$ relative to controls.

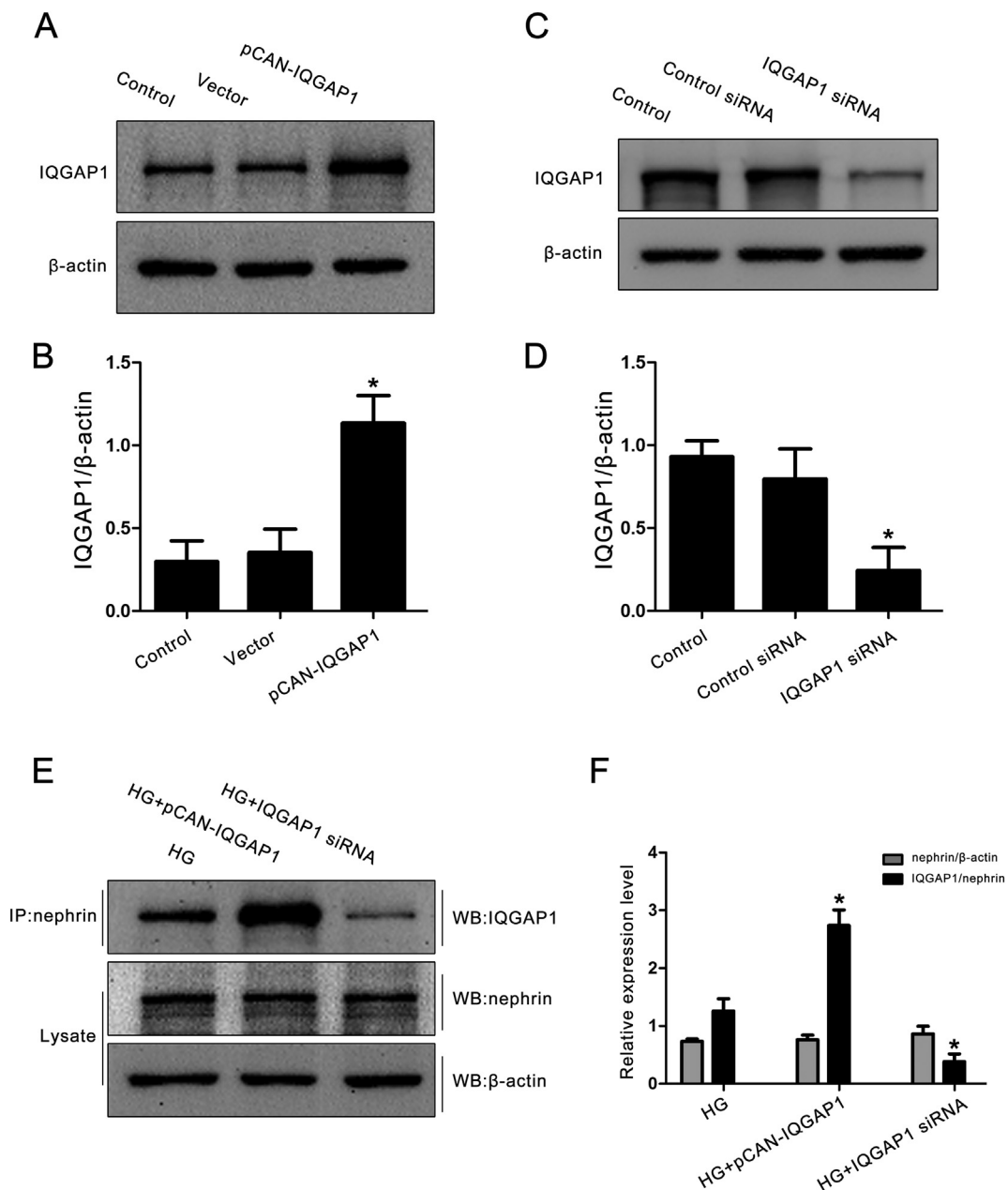


Fig. 4. Effects of IQGAP1 expression regulation on IQGAP1-nephrin interactions in podocytes. (A) (B) Western blotting analysis of IQGAP1 expression in podocytes transfected with wild-type IQGAP1 plasmid ($n = 3$). $*P < 0.05$ relative to controls. (C) (D) Western blotting analysis of IQGAP1 expression in podocytes transfected with IQGAP1 siRNA ($n = 3$). $*P < 0.05$ relative to controls. (E) (F) Western blotting analysis of nephrin and co-immunoprecipitation analysis of IQGAP1 and nephrin in podocytes stimulated by high glucose (20 mM, 40 min) and pre-transfected with IQGAP1 plasmid or siRNA ($n = 3$). $*P < 0.05$ relative to high-glucose-stimulated podocytes.

molecular transport, isolation, signal integration and transmission, protein complex assembly and so on [31–33]. IQGAP1 is the most widely distributed and deeply studied subtype of the evolutionarily conserved IQGAP scaffold protein family, and from the amino terminus to the carboxyl terminus, IQGAP1 successively contains a calponin homology domain, an IQGAP-specific repeat motif, a poly-proline binding domain (WW), a calmodulin-binding motif, a RasGTPase-activating protein-related domain (GRD), and a RasGAP domain (RGCT) that interact with many partners to participate in a variety of pathophysiological processes. Increasing studies have shown that IQGAP1 is a core regulator of endocytosis. As early as 2004, Izumi et al reported the important role of the Rac/Cdc42-IQGAP1 system in regulating E-cadherin endocytosis [34]. As the research progressed, IQGAP1 was shown to recruit β -catenin to active membrane ruffles in motile cells, where it

mediates the internalization and possible recycling of the β -catenin-associated proteins N-cadherin and APC [35]. Furthermore, IQGAP1 recruits coronin 3 and GDP-bound Rab27a to regulate the endocytosis of insulin secretory membranes [10], and IQGAP1 can cooperate with its effector mDia1 to locally stabilize microtubules and accurately localize caveolin-1 along microtubules to the cytomembrane, a process that is required for the formation of endocytic structure known as caveolae [36]. In addition, IQGAP1 can bind to transporters, such as Exo70, Sec3/8, SEPT2, Syntaxin 1A, and TSG101, and play an important role in protein transport [37]. Our previous study [14] confirmed that IQGAP1 could interact with the intracellular region of nephrin through its WW and RGCT domains and was involved in actin cytoskeleton reorganization and the functional regulation of podocytes. In the present study, we found that high-glucose levels significantly

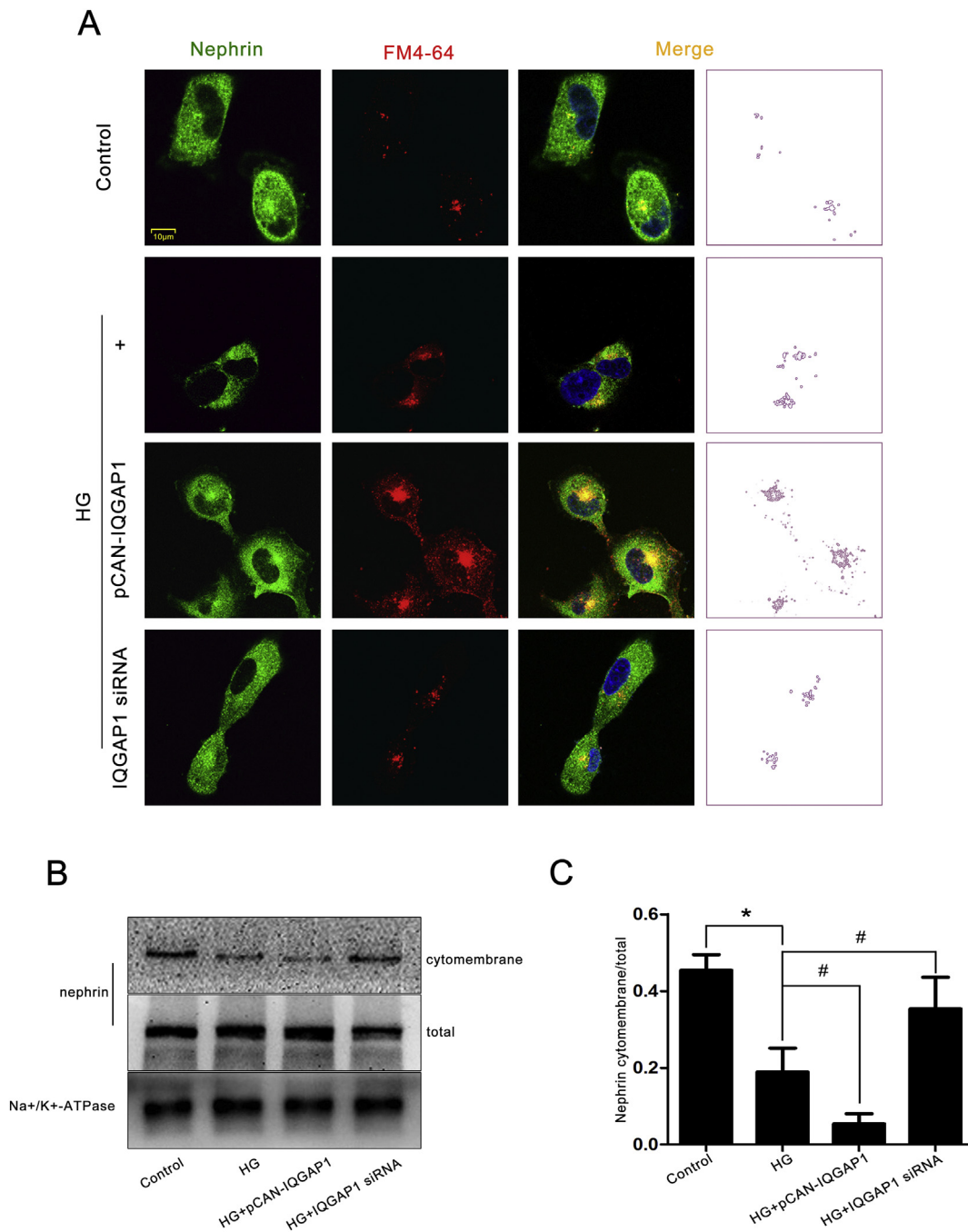


Fig. 6. Involvement of IQGAP1 in nephrin endocytosis. (A) Double immunolabelling of nephrin (green) and FM4–64 (red) in cultured podocytes stimulated with 20 mM glucose and pre-transfected with IQGAP1 siRNA or plasmid (original magnification, × 400). The area indicated by the purple dotted line is the region of nephrin and FM4–64 colocalization (yellow) presented in the third column. The nuclei were stained with DAPI (blue). Scale bar = 10 μm. (B) (C) Western blotting analysis of nephrin expression in the cytomembrane of podocytes stimulated with 20 mM glucose and pre-transfected with IQGAP1 siRNA or plasmid (n = 3). *P < 0.05 relative to controls, and #P < 0.05 relative to high-glucose-stimulated podocytes. (For interpretation of the references to colour in this figure legend, the reader is referred to the web version of this article.)

this enhanced phosphorylation leads to its reinforced interaction with nephrin. Finally, the activity of IQGAP1 as a signalling intermediate can still be controlled by regulatory protein interactions, even if the open conformation is established, as proved by its interaction with the Ca²⁺-dependent regulator calmodulin [40] and S100P [41]. The specific regulatory mechanisms in DKD still need to be studied. In this study, we also conducted a series of cell function experiments to explore the role of IQGAP1 in regulating cell migration, extensibility and permeability with high-glucose stimulation. Finally, we verified the hypothesis that IQGAP1 accumulates near the cell membrane with high-glucose

stimulation, binds to the intracellular domain of nephrin, and mediates nephrin endocytosis, which causes a decrease in nephrin levels in SDs and, eventually, podocyte injury and the appearance of proteinuria.

Despite intensive efforts, there are still some limitations within this study that must be acknowledged. First, phospho-regulation of nephrin has been reported to participate in podocyte survival, cytoskeletal regulation and membrane trafficking [22]. Whether nephrin phosphorylation initiates the process of IQGAP1-mediated endocytosis, which residue is specifically phosphorylated, and which phosphatase catalyses this process are unknown. Second, the exact mechanism

regulating the interaction between IQGAP1 and nephrin in DKD remains unclear. Third, there are two principal endocytic pathways in podocytes: clathrin-mediated endocytosis and clathrin-independent, raft-mediated endocytosis [27]; the specific pathway involved in nephrin internalization in DKD still needs to be further explored. Finally, endocytosis is a complex process. The post-endocytic trafficking of nephrin and the other involved molecules have not been fully characterized. More in-depth research will be implemented in the future to answer the above questions.

To the best of our knowledge, this was the first study to assess the regulatory role of IQGAP1 in mediating nephrin endocytosis in DKD. Here, we verified that IQGAP1, an intracellular partner of nephrin, participates in the control of nephrin endocytosis and functional regulation of podocytes in DKD. Our finding suggested that IQGAP1-mediated nephrin endocytosis may be one of the critical molecular pathophysiology way of DKD. However, further detailed studies are required to pinpoint the underlying regulatory mechanisms both *in vivo* and *in vitro*.

Supplementary data to this article can be found online at <https://doi.org/10.1016/j.cellsig.2019.03.009>.

Author contributions

YL and DX conceived the project. YL, CM, DJ, XZ and DX designed experiments. YL, HS, PW, SZ, LW and ZW carried out experiments. YL, HS, PW and DX analysed data. YL and HS wrote the paper with input from all authors.

Acknowledgments

This work was supported by the National Natural Science Foundation of China (81500555) to Y. L., the Third Project of Jinan City Science and Technology Development Plan (201503002) to Y. L. and Young Taishan Scholars Program.

Declarations of interest

None.

References

1. A. Menke, S. Casagrande, L. Geiss, C.C. Cowie, Prevalence of and trends in diabetes among adults in the United States, 1988–2012, *Jama* 314 (2015) 1021–1029.
2. L.C. Plantinga, D.C. Crews, J. Coresh, E.R. Miller 3rd, R. Saran, J. Yee, E. Hedgeman, M. Pavkov, M.S. Eberhardt, D.E. Williams, N.R. Powe, Team CCS, Prevalence of chronic kidney disease in US adults with undiagnosed diabetes or prediabetes, *Clin. J. Am. Soc. Nephrol.* 5 (2010) 673–682.
3. M. Afkarian, M.C. Sachs, B. Kestenbaum, I.B. Hirsch, K.R. Tuttle, J. Himmelfarb, I.H. de Boer, Kidney disease and increased mortality risk in type 2 diabetes, *J. Am. Soc. Nephrol.* 24 (2013) 302–308.
4. M. Nagata, Podocyte injury and its consequences, *Kidney Int.* 89 (2016) 1221–1230.
5. V.D. D'Agati, F.J. Kaskel, R.J. Falk, Focal segmental glomerulosclerosis, *N. Engl. J. Med.* 365 (2011) 2398–2411.
6. G.I. Welsh, M.A. Saleem, Nephrin-signature molecule of the glomerular podocyte? *J. Pathol.* 220 (2010) 328–337.
7. J. Patrakka, K. Tryggvason, Nephrin—a unique structural and signaling protein of the kidney filter, *Trends Mol. Med.* 13 (2007) 396–403.
8. K. Inoki, H. Mori, J. Wang, T. Suzuki, S. Hong, S. Yoshida, S.M. Blattner, T. Ikenoue, M.A. Ruegg, M.N. Hall, D.J. Kwiatkowski, M.P. Rastaldi, T.B. Huber, M. Kretzler, L.B. Holzman, R.C. Wiggins, K.L. Guan, mTORC1 activation in podocytes is a critical step in the development of diabetic nephropathy in mice, *J. Clin. Invest.* 121 (2011) 2181–2196.
9. I. Tossidou, B. Teng, J. Menne, N. Shushakova, J.K. Park, J.U. Becker, F. Modde, M. Leitges, H. Haller, M. Schiffer, Podocytic PKC- α is regulated in murine and human diabetes and mediates nephrin endocytosis, *PLoS ONE* 5 (2010) e10185.
10. T. Kimura, M. Yamaoka, S. Taniguchi, M. Okamoto, M. Takei, T. Ando, A. Iwamatsu, T. Watanabe, K. Kaibuchi, T. Ishizaki, I. Niki, Activated Cdc42-bound IQGAP1 determines the cellular endocytic site, *Mol. Cell. Biol.* 33 (2013) 4834–4843.
11. P. Arpitha, C.Y. Gao, B.K. Tripathi, S. Saravanamuthu, P. Zelenka, Cyclin-dependent kinase 5 promotes the stability of corneal epithelial cell junctions, *Mol. Vis.* 19 (2013) 319–332.
12. S. Lehtonen, J.J. Ryan, K. Kudlicka, N. Iino, H. Zhou, M.G. Farquhar, Cell junction-associated proteins IQGAP1, MAGI-2, CASK, spectrins, and alpha-actinin are components of the nephrin multiprotein complex, *Proc. Natl. Acad. Sci. U. S. A.* 102 (2005) 9814–9819.
13. X.L. Liu, P. Kilpelainen, U. Hellman, Y. Sun, J. Wartiovaara, E. Morgunova, T. Pikkarainen, K. Yan, A.P. Jonsson, K. Tryggvason, Characterization of the interactions of the nephrin intracellular domain, *FEBS J.* 272 (2005) 228–243.
14. Y. Liu, W. Liang, Y. Yang, Y. Pan, Q. Yang, X. Chen, P.C. Singhal, G. Ding, IQGAP1 regulates actin cytoskeleton organization in podocytes through interaction with nephrin, *Cell. Signal.* 27 (2015) 867–877.
15. M. Liu, K. Liang, J. Zhen, M. Zhou, X. Wang, Z. Wang, X. Wei, Y. Zhang, Y. Sun, Z. Zhou, H. Su, C. Zhang, N. Li, C. Gao, J. Peng, F. Yi, Sirt6 deficiency exacerbates podocyte injury and proteinuria through targeting notch signaling, *Nat. Commun.* 8 (2017) 413.
16. X. Wang, J. Liu, J. Zhen, C. Zhang, Q. Wan, G. Liu, X. Wei, Y. Zhang, Z. Wang, H. Han, H. Xu, C. Bao, Z. Song, X. Zhang, N. Li, F. Yi, Histone deacetylase 4 selectively contributes to podocyte injury in diabetic nephropathy, *Kidney Int.* 86 (2014) 712–725.
17. Q. Wan, Y. Xu, E. Dong, Diabetic nephropathy research in China: data analysis and review from the National Natural Science Foundation of China, *J. Diabetes* 7 (2015) 307–314.
18. J. Reiser, S. Sever, Podocyte biology and pathogenesis of kidney disease, *Annu. Rev. Med.* 64 (2013) 357–366.
19. H. Dai, Q. Liu, B. Liu, Research progress on mechanism of podocyte depletion in diabetic nephropathy, *J. Diabetes Res.* 2017 (2017) 2615286.
20. A. Swiatecka-Urban, Endocytic trafficking at the mature podocyte slit diaphragm, *Front. Pediatr.* 5 (2017) 32.
21. M. Ristola, S. Lehtonen, Functions of the podocyte proteins nephrin and Neph3 and the transcriptional regulation of their genes, *Clin. Sci.* 126 (2014) 315–328.
22. C.E. Martin, N. Jones, Nephrin signaling in the podocyte: an updated view of signal regulation at the slit diaphragm and beyond, *Front. Endocrinol.* 9 (2018) 302.
23. B. Teng, P. Schroder, J. Muller-Deile, H. Schenk, L. Staggs, I. Tossidou, I. Dikic, H. Haller, M. Schiffer, CIN85 deficiency prevents nephrin endocytosis and proteinuria in diabetes, *Diabetes* 65 (2016) 3667–3679.
24. C.E. Martin, K.A. Petersen, L. Aoudjit, M. Tilak, V. Eremina, W.R. Hardy, S.E. Quaggin, T. Takano, N. Jones, ShcA adaptor protein promotes nephrin endocytosis and is upregulated in proteinuric nephropathies, *J. Am. Soc. Nephrol.* 29 (2018) 92–103.
25. Y. Nishibori, L. Liu, M. Hosoyamada, H. Endou, A. Kudo, H. Takenaka, E. Higashihara, F. Bessho, S. Takahashi, D. Kershaw, V. Ruotsalainen, K. Tryggvason, J. Khoshnoodi, K. Yan, Disease-causing missense mutations in NPHS2 gene alter normal nephrin trafficking to the plasma membrane, *Kidney Int.* 66 (2004) 1755–1765.
26. K. Inoue, S. Ishibe, Podocyte endocytosis in the regulation of the glomerular filtration barrier, *Am. J. Physiol. Ren. Physiol.* 309 (2015) F398–F405.
27. K. Soda, S. Ishibe, The function of endocytosis in podocytes, *Curr. Opin. Nephrol. Hypertens.* 22 (2013) 432–438.
28. A.M. Waters, M.Y. Wu, Y.W. Huang, G.Y. Liu, D. Holmyard, T. Onay, N. Jones, S.E. Egan, L.A. Robinson, T.D. Piscione, Notch promotes dynamin-dependent endocytosis of nephrin, *J. Am. Soc. Nephrol.* 23 (2012) 27–35.
29. E. Konigshausen, U.M. Zierhut, M. Ruetze, S.A. Potthoff, J. Stegbauer, M. Woznowski, I. Quack, L.C. Rump, L. Sellin, Angiotensin II increases glomerular permeability by beta-arrestin mediated nephrin endocytosis, *Sci. Rep.* 6 (2016) 39513.
30. V. Dumont, T.A. Tolvanen, S. Kuusela, H. Wang, T.A. Nyman, S. Lindfors, J. Tienari, H. Nisen, S. Suetsugu, M. Plomann, H. Kawachi, S. Lehtonen, PACSIN2 accelerates nephrin trafficking and is up-regulated in diabetic kidney disease, *FASEB J.* 31 (2017) 3978–3990.
31. S. Malarkannan, A. Awasthi, K. Rajasekaran, P. Kumar, K.M. Schuldt, A. Bartoszek, N. Manoharan, N.K. Goldner, C.M. Umhoefer, M.S. Thakar, IQGAP1: a regulator of intracellular spacetime relativity, *J. Immunol.* 188 (2012) 2057–2063.
32. A.C. Hedman, J.M. Smith, D.B. Sacks, The biology of IQGAP proteins: beyond the cytoskeleton, *EMBO Rep.* 16 (2015) 427–446.
33. T. Watanabe, S. Wang, K. Kaibuchi, IQGAPs as key regulators of actin-cytoskeleton dynamics, *Cell Struct. Funct.* 40 (2015) 69–77.
34. G. Izumi, T. Sakisaka, T. Baba, S. Tanaka, K. Morimoto, Y. Takai, Endocytosis of E-cadherin regulated by Rac and Cdc42 small G proteins through IQGAP1 and actin filaments, *J. Cell Biol.* 166 (2004) 237–248.
35. M. Sharma, B.R. Henderson, IQ-domain GTPase-activating protein 1 regulates beta-catenin at membrane ruffles and its role in macropinocytosis of *N-cadherin* and adenomatous polyposis coli, *J. Biol. Chem.* 282 (2007) 8545–8556.
36. S.A. Wickstrom, A. Lange, M.W. Hess, J. Polleux, J.P. Spatz, M. Kruger, K. Pfaller, A. Lambacher, W. Bloch, M. Mann, L.A. Huber, R. Fassler, Integrin-linked kinase controls microtubule dynamics required for plasma membrane targeting of caveolae, *Dev. Cell* 19 (2010) 574–588.
37. C.D. White, H.H. Erdemir, D.B. Sacks, IQGAP1 and its binding proteins control diverse biological functions, *Cell. Signal.* 24 (2012) 826–834.
38. I. Quack, M. Woznowski, S.A. Potthoff, R. Palmer, E. Konigshausen, S. Sivritas, M. Schiffer, J. Stegbauer, O. Vonend, L.C. Rump, L. Sellin, PKC alpha mediates beta-arrestin2-dependent nephrin endocytosis in hyperglycemia, *J. Biol. Chem.* 286 (2011) 12959–12970.
39. K. Grohmanova, D. Schlaepfer, D. Hess, P. Gutierrez, M. Beck, R. Kroschewski, Phosphorylation of IQGAP1 modulates its binding to Cdc42, revealing a new type of rho-GTPase regulator, *J. Biol. Chem.* 279 (2004) 48495–48504.
40. Z. Li, D.B. Sacks, Elucidation of the interaction of calmodulin with the IQ motifs of IQGAP1, *J. Biol. Chem.* 278 (2003) 4347–4352.
41. A. Heil, A.R. Nazmi, M. Koltzsch, M. Poeter, J. Austermann, N. Assard, J. Baudier, K. Kaibuchi, V. Gerke, S100P is a novel interaction partner and regulator of IQGAP1, *J. Biol. Chem.* 286 (2011) 7227–7238.